

Supporting information

Hydrophobized Plant Polyphenol: Self-Assembly and Promising Antibacterial, Adhesive, and Anticorrosion Coatings

Debabrata Payra,^a Masanobu Naito,*^a Yoshihisa Fujii,^b and Yuki Nagao^c

^a *Research Center for Strategic Materials, Structural Materials Unit, National Institute for Materials Science (NIMS), 1-1 Namiki, Tsukuba, Ibaraki 305-0044, Japan*

^b *Advanced Key Technologies Division, Polymer Materials Unit, National Institute for Materials Science (NIMS), 1-1 Namiki, Tsukuba, Ibaraki 305-0044, Japan*

^c *School of Materials Science, Japan Advanced Institute of Science, and Technology, 1-1 Asahidai, Nomi, Ishikawa 923-1292, Japan*

For all correspondence: NAITO.Masanobu@nims.go.jp

Contents

1. General information.....	S2-S3
2. Synthesis.....	S4
3. Characterization and physical properties.....	S5-S10
4. Thin-film properties.....	S11-S16
5. Anti-corrosion tests.....	S17-S19
6. Anti-bacterial test.....	S20
7. References.....	S21

1. General Information

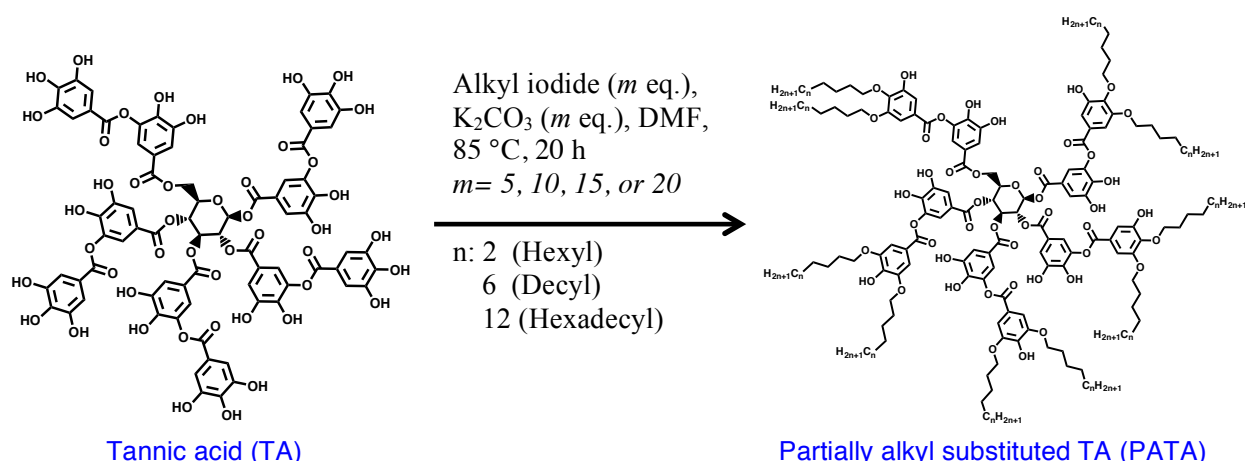
Materials: All manipulations were carried out under argon atmosphere employing standard Schlenk techniques. Ultrapure water (resistivity=18.2 M Ω , pH = 6.82) used in all experiments was obtained from a Millipore. Tannic acid (TA) was purchased from Wako chemicals, alkyl (hexyl, decyl, and hexadecyl) iodides from Tokyo Chemical Industry Co. Ltd. (TCI), and other chemicals/solvents were from commercial sources and used without further purification.

Instrumentation:

- a. **NMR & FT-IR:** ^1H NMR spectra were measured for $\text{C}_2\text{D}_6\text{SO}$ (containing 1% TMS) solutions at 25 °C on JEOL JNM-ECX 300 spectrometer and the chemical shifts are reported in ppm with respect to the reference SiMe_4 . FT-IR was measured for KBr pellet in a JASCO FT-IR 6100 instrument.
- b. **TGA & DSC:** Thermogravimetric analysis (TGA) and differential scanning calorimetry (DSC) were studied using SII Seiko instruments TG/DTA 6200 and X-DSC 7000, respectively. Aluminum pan was used as a sample holder and alumina (Al_2O_3) powder was used a reference for all cases. Heating rate was 10 °C/min for both analysis. The second heating/cooling cycle is reported in all cases of DSC to avoid impurity/solvent peak.
- c. **Surface profiler & Contact angle:** Thin-film thickness was measured by a DEKTAK 6M Stylus surface profiler. Reported thicknesses are average of 5-6 measurements for each sample. Static water contact angle of coated glass surface was measured using Dropmaster 300 instrument at 298 K. Reported contact angles are average of 5-6 measurements.
- d. **AFM & SEM:** Atomic force microscopy (AFM) was studied using NanoNavi SII instrument. Scanning electron microscope (SEM) was studied by Hitachi SU4800/ 8000 instrument. Samples were Pt coated for 30 s in all cases.
- e. **Thin-film XRD & WAXD:** Thin-film X-ray diffraction (XRD) was measured using SmartLab apparatus and the film was made on a cover slip by simple drop-casting method followed by solvent evaporation under ambient condition or annealing at 80°C for 1 h. Wide-angle X-ray diffraction (WAXD) experiments in out-of-plane geometry were carried out with a Rigaku Smartlab using $\text{CuK}\alpha$ radiation. These data were collected with the angular interval between steps 0.08 ° and a scan speed of 0.5 ° per min.
- f. **Electro-polarization and salt-water immersion test:** Anti-corrosion study by electrochemical method was done using ALS-CHI 660A electrochemical set up having four electrodes com-

binations. Metal/alloy rods were cut into small plates of 2 mm thickness, polished with SiC paper, and cleaned according to a previous report.^a Coated/uncoated Mg substrates were used as working electrode, standard calomel electrode as reference electrode, platinum foil connected with a wire as counter electrode and sense. Before final measurement, all samples were immersed in 3.5 wt.% NaCl solution for 1 h. Open circuit potential was monitored for 10 min for each case to reach an electrochemical steady state. Finally, cathodic/anodic current were measured independently at a scan rate of 1 mV/s. Salt-water immersion test was studied for all samples in 3.5 wt.% NaCl aq. solution at room temperature. Al (99%, Nilaco Corp.), Cu (99.9%, Nilaco Corp.), Fe (3N5 purity, ESPI), Zn (6N purity, ESPI), and Mg (AZ31) were used in this study. Schematic diagrams of these tests have been shown in Figure S14.

2. Synthesis



Scheme S1: Chemical modification of tannic acid (TA). Incorporation of different alkyl chains (hexyl, decyl or hexadecyl) to the TA backbone was done in the presence of potassium carbonate.

TA (1 gm., 0.587 mmol) and K_2CO_3 (m eq.) was mixed in a two-necked round bottom flask fitted with a water condenser. Flask was back-filled with argon twice and dimethylformamide (DMF, 15 mL) was added to the solid mixture. After shaking/stirring the reaction mixture for 10-15 minutes, alkyl iodide (m eq.) was added to the reaction mixture by a syringe at room temperature and reaction mixture was stirred vigorously at 85°C for 20 h. Finally, dark brown reaction mixture was cooled down to room temperature, solid residue was filtered out by simple filtration and washed few times with DMF. Collected filtrate was mixed together and most of the solvent was removed by high vacuum at 50°C . Excess amount of distilled water was added to the concentrated reaction mixture and vigorously stirred using a vortex mixing equipment. After 1 h, solid precipitate/sticky material was isolated by simple filtration/centrifugation. Solid materials were further dissolved in excess chloroform (~ 150 mL) by gentle heating/sonication and dried over sodium sulfate. After filtration and washing several times with chloroform, organic solvent was removed by a rotary evaporator. Dark brown product was further dried under high vacuum at 45°C for 10 h.

Compound	Alkyl iodide (wt.%)	TA (wt.%)	Aromatic -OH converted (mol %)	Yield (%)
TA(C ₆) ₅	C ₆ H ₁₃ I (38)	62	20	73
TA(C ₆) ₁₀	C ₆ H ₁₃ I (55)	45	40	87
TA(C ₁₀) ₅	C ₁₀ H ₂₁ I (44)	56	20	88
TA(C ₁₀) ₁₀	C ₁₀ H ₂₁ I (61)	39	40	74
TA(C ₁₀) ₁₅	C ₁₀ H ₂₁ I (70)	30	60	76
TA(C ₁₀) ₂₀	C ₁₀ H ₂₁ I (76)	24	80	94
TA(C ₁₆) ₅	C ₁₆ H ₃₃ I (51)	49	20	72
TA(C ₁₆) ₁₀	C ₁₆ H ₃₃ I (67)	33	40	61

Table S1: Various composition and combination of alkyl iodide and TA with different weight ratios.

3. Characterization and physical properties

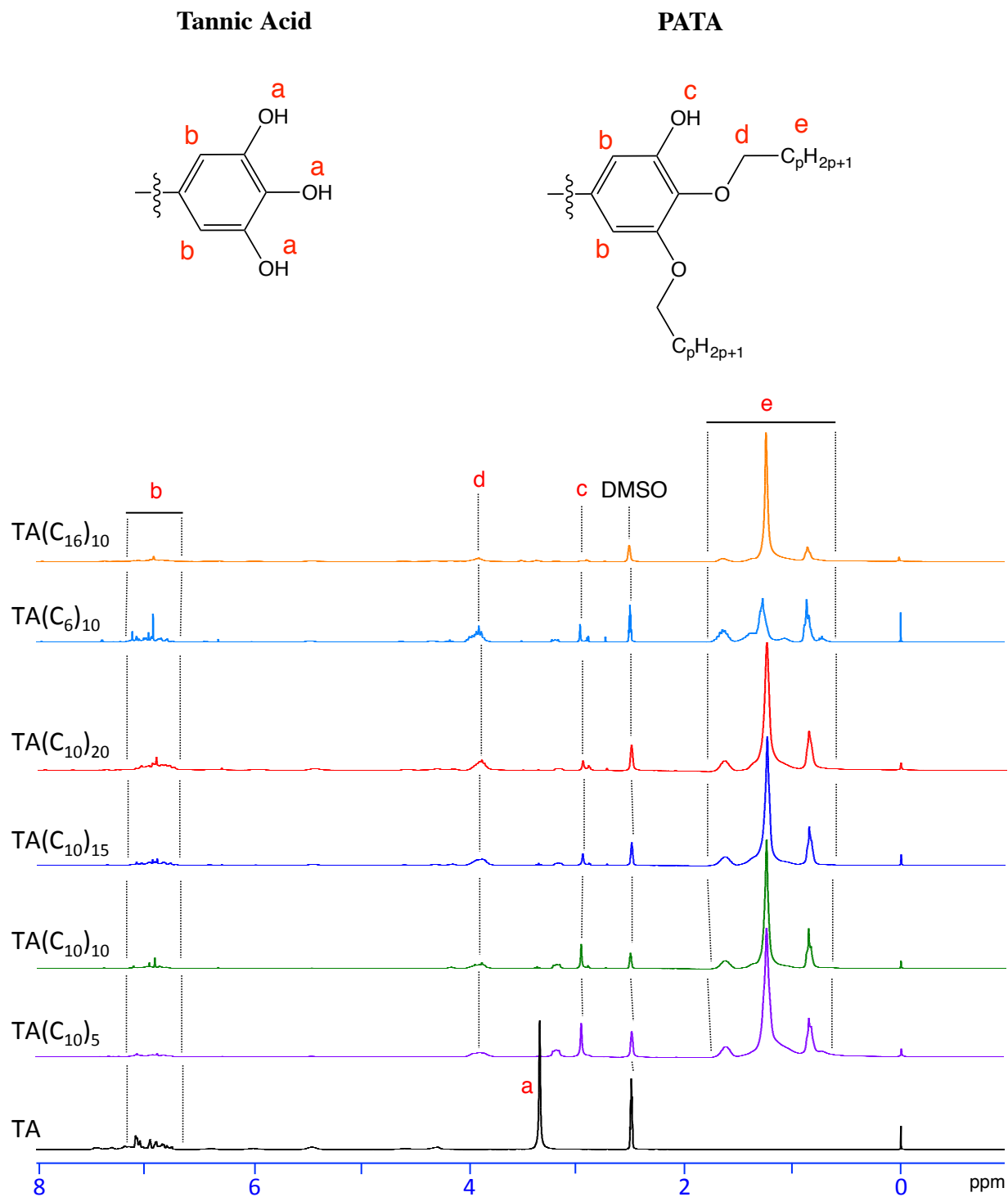


Figure S1: ¹H NMR comparison among TA and PATAs in DMSO at 298K. Appearance of multiple broad peaks around 0.8~1.5 ppm indicate incorporation of alkyl chains to the TA backbone. In addition, appearance of peak around 4 ppm indicates formation of ether (–OCH₂–) linkages.

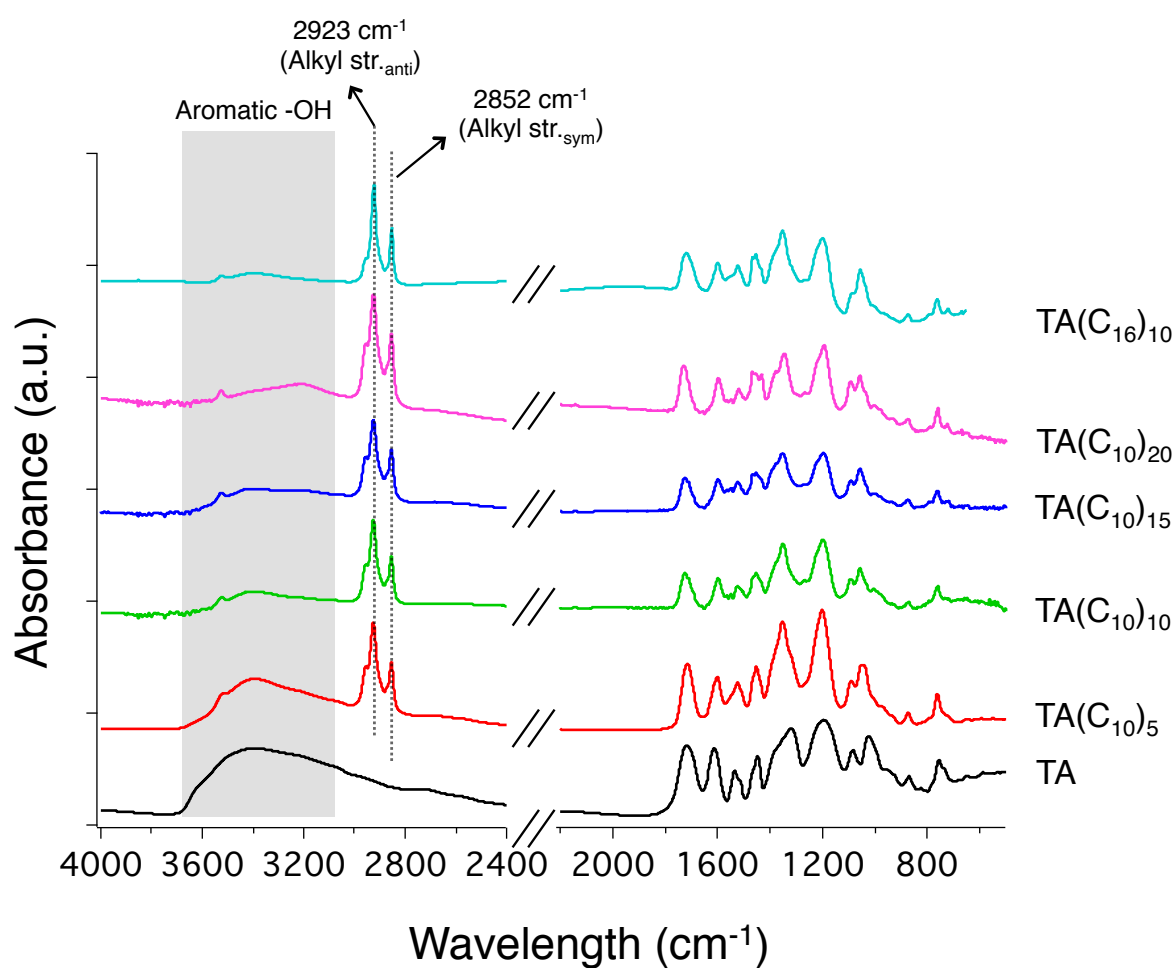


Figure S2: FT-IR comparison among TA and PATAs in KBr pellet. Gradual decrease of aromatic hydroxyls broad peak (3100~3600 cm⁻¹) and appearance of typical alkyl -CH₂ & -CH₃ signals (~2800-2950 cm⁻¹) indicate conversion of aromatic hydroxyls to ether linkages.

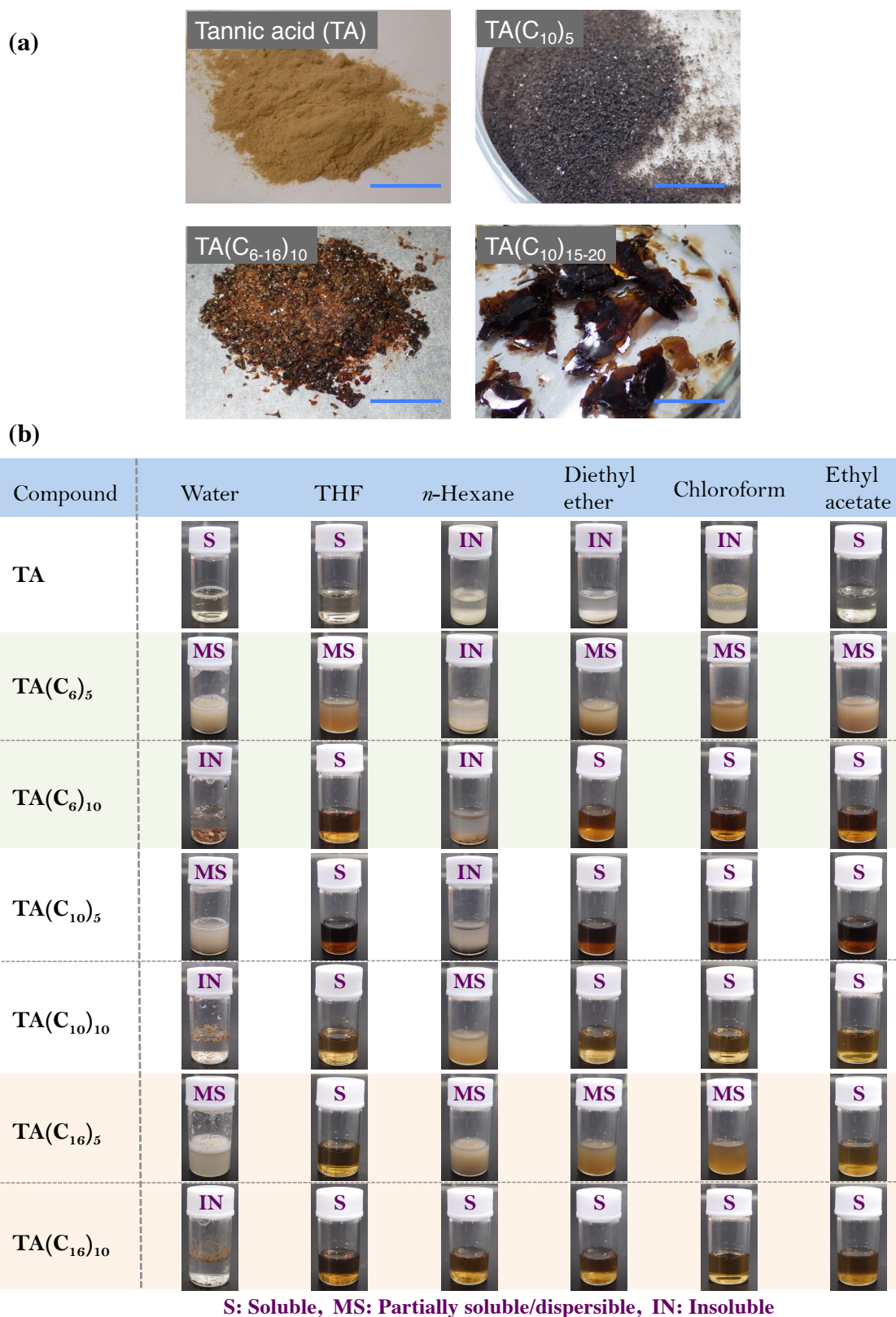


Figure S3: (a) Comparison of physical appearance before and after alkyl substitutions. TA appears as a yellow powder while, turns to dark brown shiny materials after alkylation. Image scale bar is 1 cm. (b) Comparison of solubility in water and different organic media. Obviously, partial alkylation significantly improves organosolubility of TA.

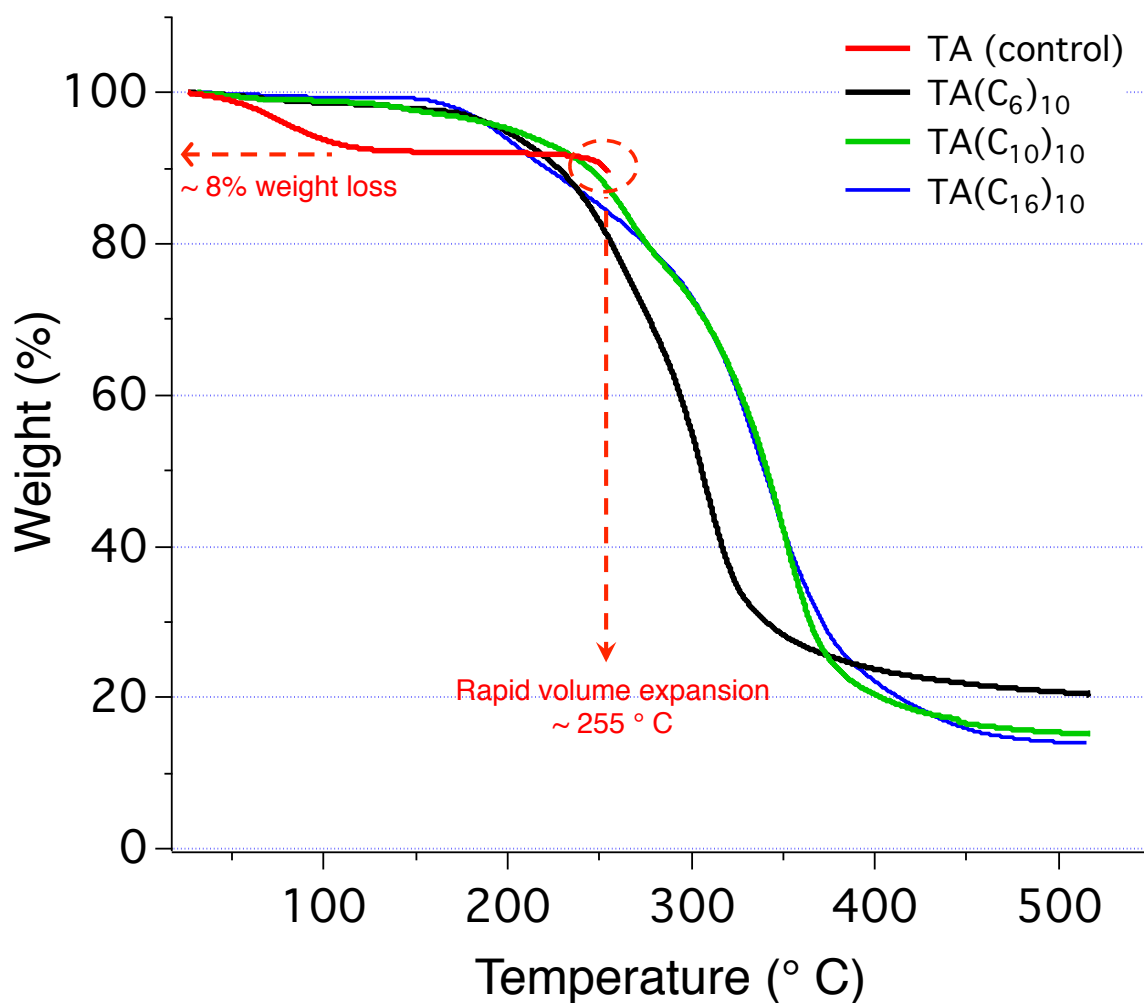


Figure S4: Thermo gravimetric analysis (TGA) plots of pristine TA and PATAs. Commercially available TA powder was used for this study without further purification. There was a rapid volume expansion for TA after 255 °C, which caused falling the sample pan from holder (red line). Therefore, correct measurement of weight loss above this temperature was difficult. Further, we observed about 8% weight loss in between 50-100 °C for commercially available TA sample, possibly due to low molecular weight or other foreign species. In contrast, these phenomena were not detected after introducing long alkyl units to the TA backbone and PATAs were thermally stable at least upto 180 °C (black, green, and blue line). However, gradual weight loss was observed for PATA samples above ca. 200 °C, and ~80% decomposition was recorded above 350 °C.

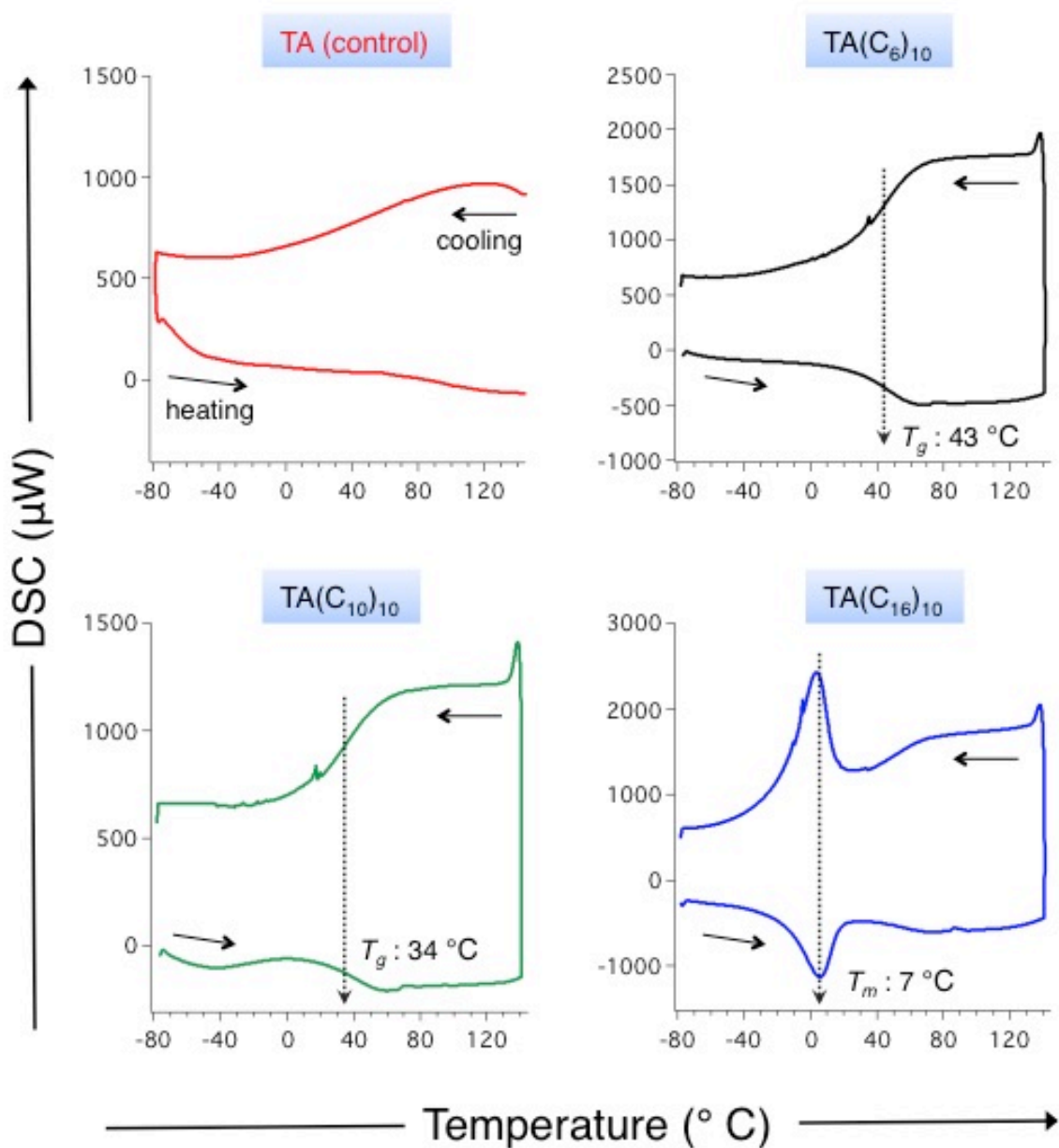


Figure S5: Differential scanning calorimetry (DSC) thermograms of TA and PATAs. Pristine TA does not have significant phase transition in the observed temperature range (red plot). However, PATAs have distinct transition depending on the type of alkyl side chains. For example, hexyl and decyl substituted samples show a glass transition (T_g) close to 43 °C and 34 °C, respectively (black & green plot). More longer alkyl unit (C_{16}) substituted sample shows a distinct melting point (T_m) close to 7 °C (blue plot). These phenomena clearly indicate the change and dependence of intra-/intermolecular physical interaction in solid phase with the incorporation of soft alkyl chain brushes.

Molecular simulation :

Density functional theory (DFT) calculations were performed using the DMol3 package in Materials Studio v7.0 (Accelrys Software). The Perdew–Burke–Ernzerhof (PBE) function was chosen. The convergence threshold for the maximum force and maximum displacement for normal geometry optimization were set, respectively, to $0.02 \text{ Ha } \text{\AA}^{-1}$ and 0.05 \AA .

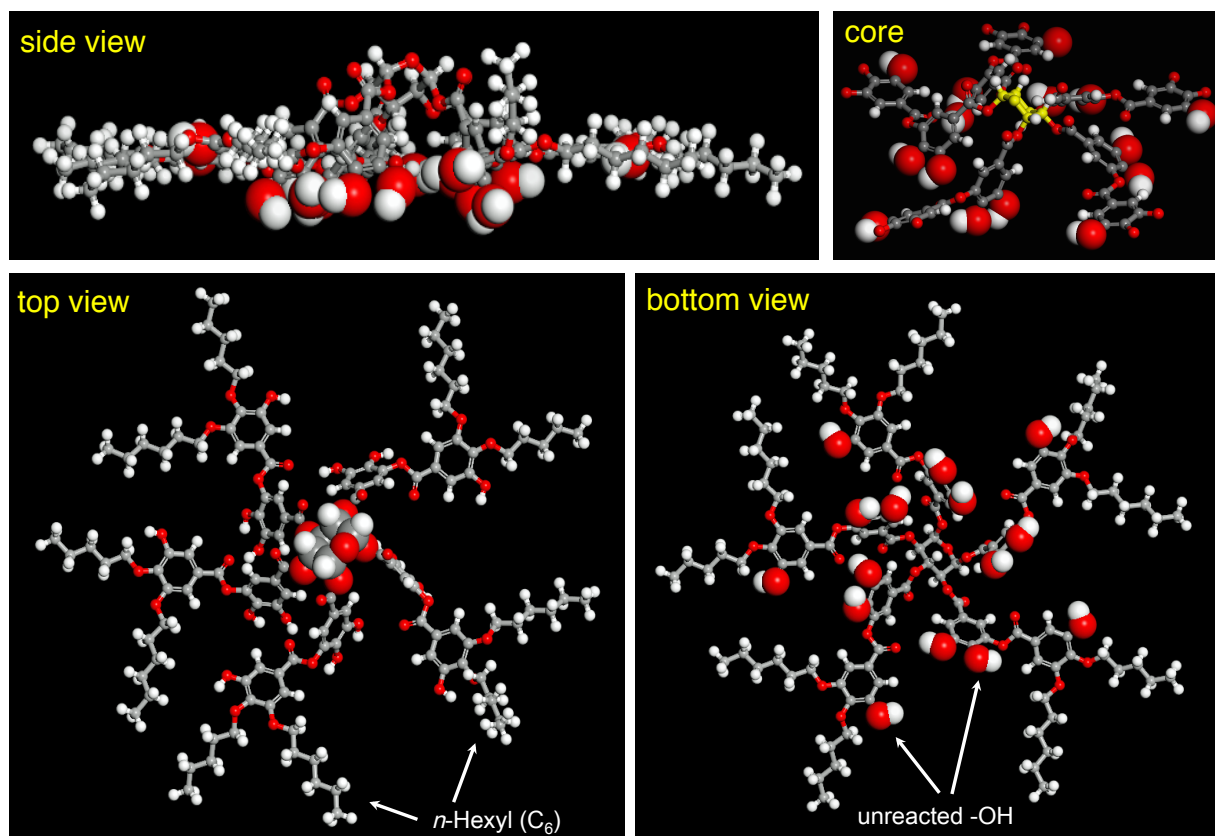


Figure S6: Most stable molecular structure of PATA as estimated by DFT. For clarity, aromatic hydroxyls of the most outer ring were substituted by ten *n*-hexyl alkyl chains. The glucose core was preferably in chair conformation and alkyl units were surrounded like a disc-like molecular structure.

4. Thin-film properties

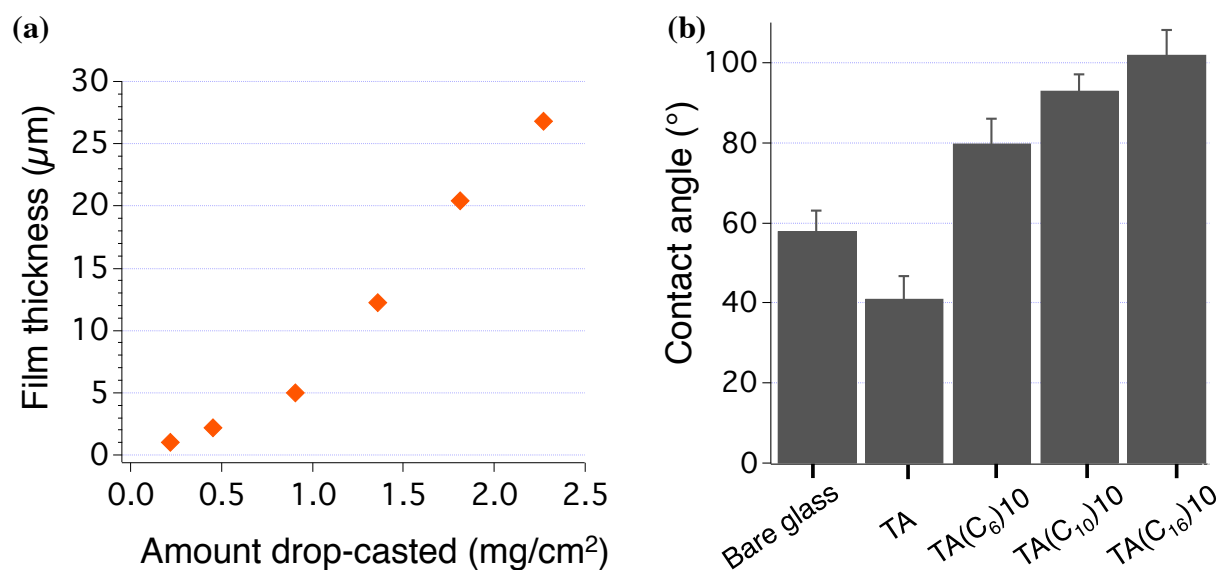


Figure S7: (a) Relation between amount drop-casted and film thickness. (b) Comparison of static water contact angle among different (un)coated glass surfaces. TA coated surface is hydrophilic while, PATAs were relatively hydrophobic which is reasonable for the incorporation of long alkyl chains to TA backbone.

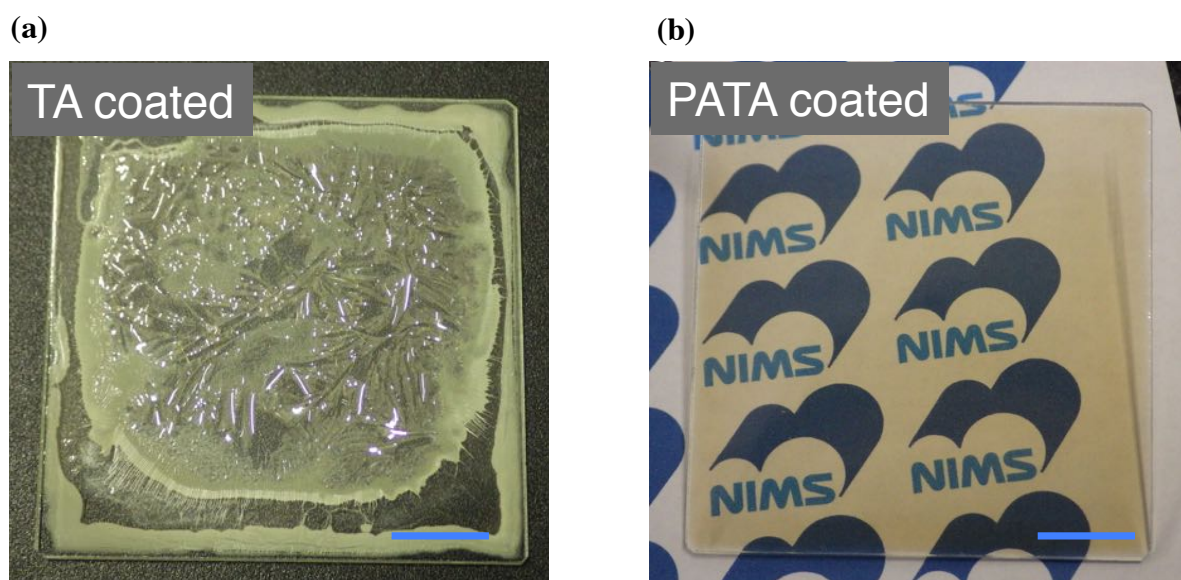


Figure S8: Photographs of (a) TA coated, and (b) PATA coated glass plate. Distinctly, film of pristine TA was unstable under ambient condition but PATA film was smooth, stable, and uniform on glass surface. Image scale bar is 1 cm.

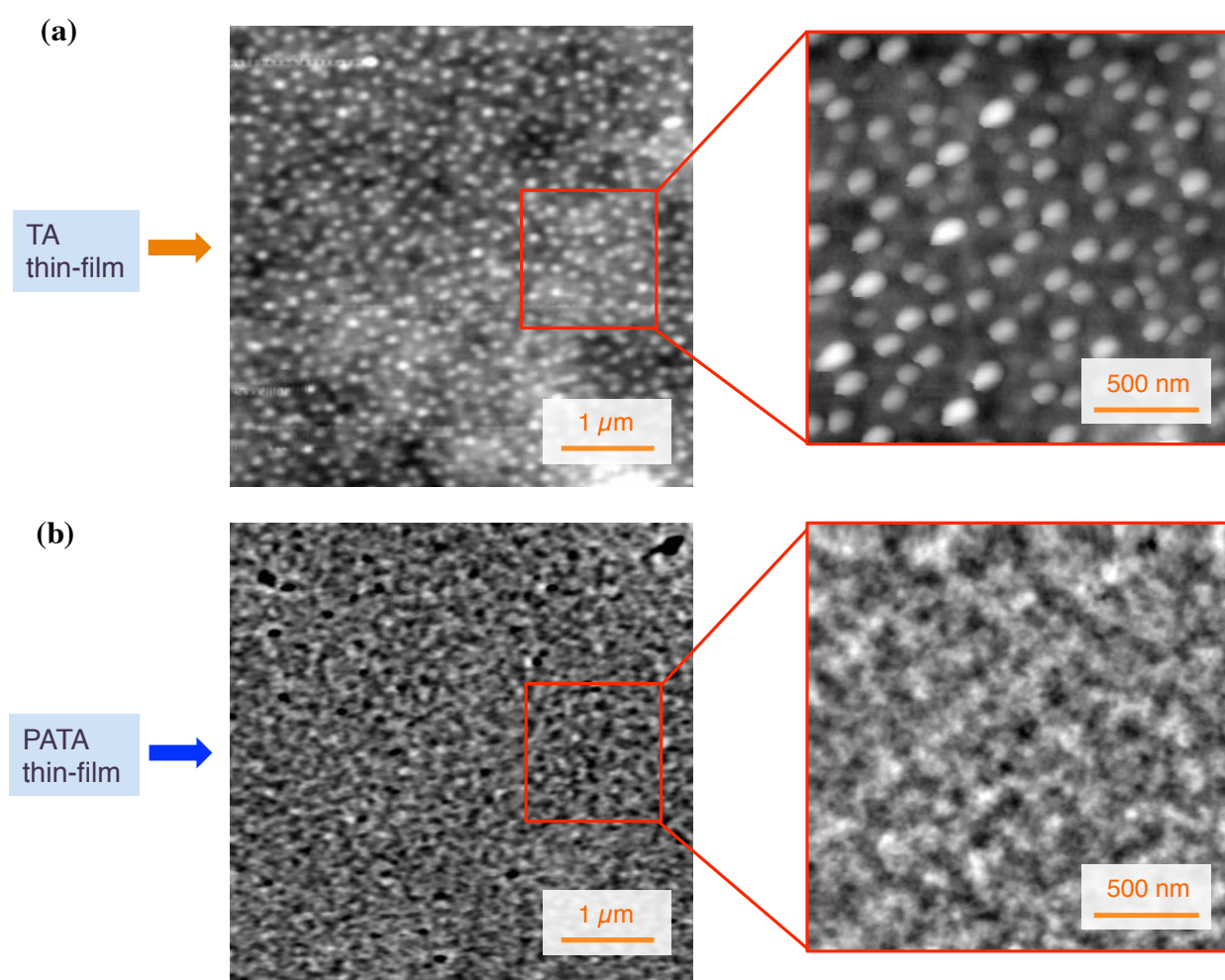


Figure S9: Atomic force microscope (AFM) phase images of (a) TA film, and (b) TA(C₁₆)₁₀ film on glass surface. Average particle size of TA aggregates was 100-130 nm. On the contrary, TA(C₁₆)₁₀ film produced a uniform fibre-like network assembly. These figures clarify that TA aggregates to a particle morphology possibly due to random intra-/intermolecular hydrogen bonding among aromatic ester/hydroxyls groups. However, alkyl substitutions give network assembly via intramolecular hydrophobic interactions.

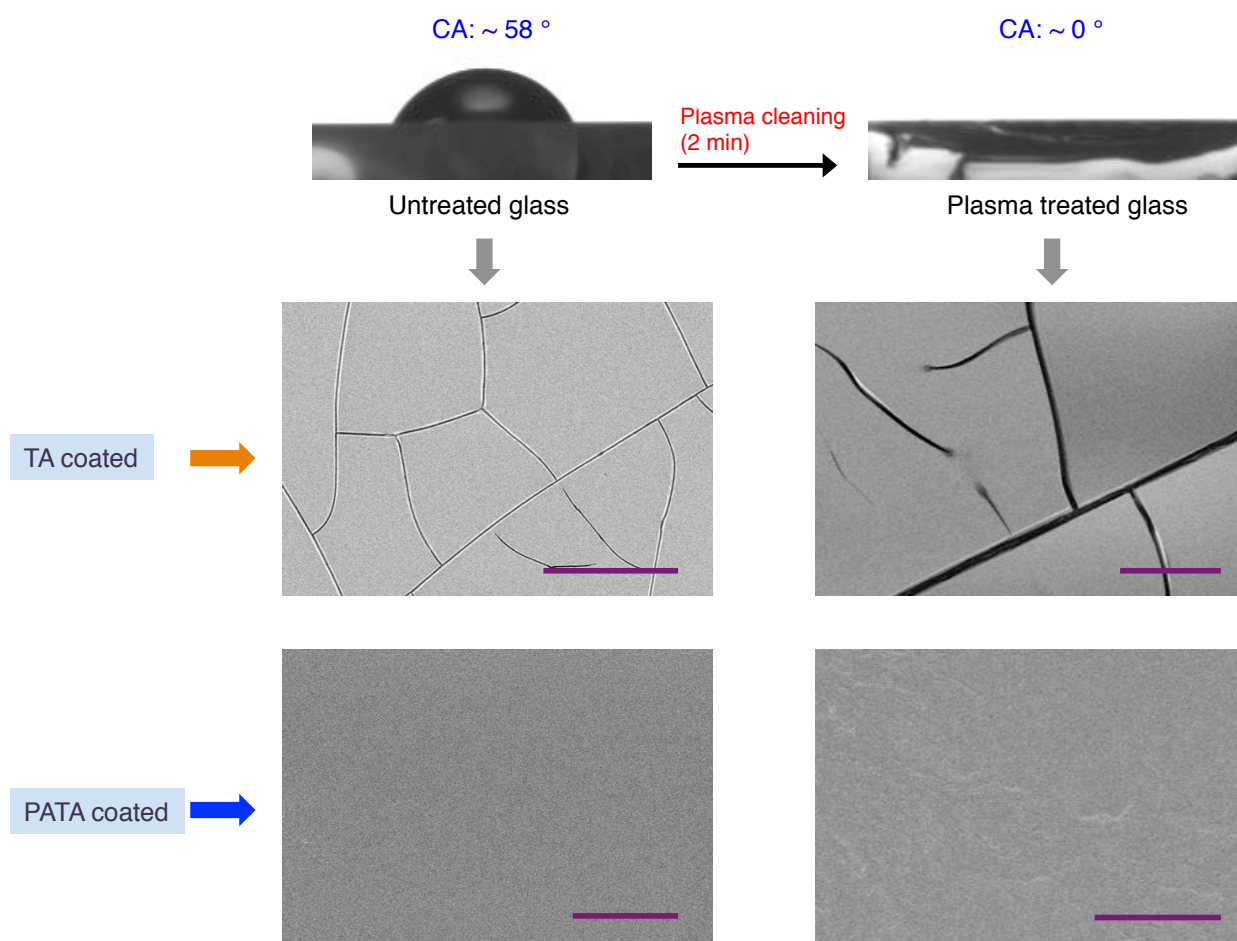
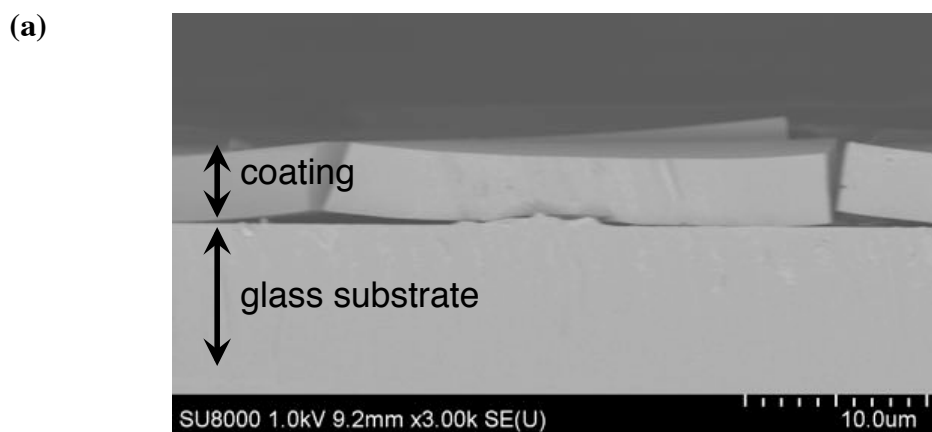


Figure S10: Top surface scanning electron microscope (SEM) images of TA (control) and TA(C₁₆)₁₀ film. We verified thin-film morphology on both untreated glass (hydrophobic) and plasma treated glass (hydrophilic). Obviously, TA film has many cracks formed possibly during solvent evaporation process and indicate poor film stability on both (hydro)phobic/philic surfaces. On the other hand, TA(C₁₆)₁₀ coated film was smooth, crack-free, and well-adhered to the surface indicating good film stability. Therefore, we believe defect in TA film is not due to weak TA/glass interaction but due to poor intramolecular interactions. Hydrophobization of TA helps to overcome this drawback by stronger alkyl-alkyl hydrophobic interactions. Scale bar of the images are 10 μm .

TA film (control)



PATA film

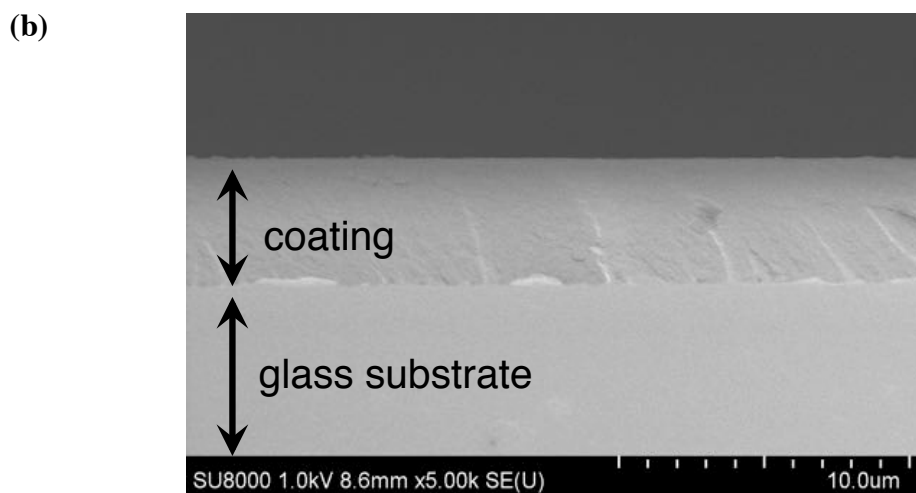


Figure S11: Cross-sectional SEM images of (a) TA (control) and (b) TA(C₁₆)₁₀ film. TA film was cracked and peeled-off from the glass surface but TA(C₁₆)₁₀ coated film was well-adhered to the surface indicating good anchoring and mechanical stability.

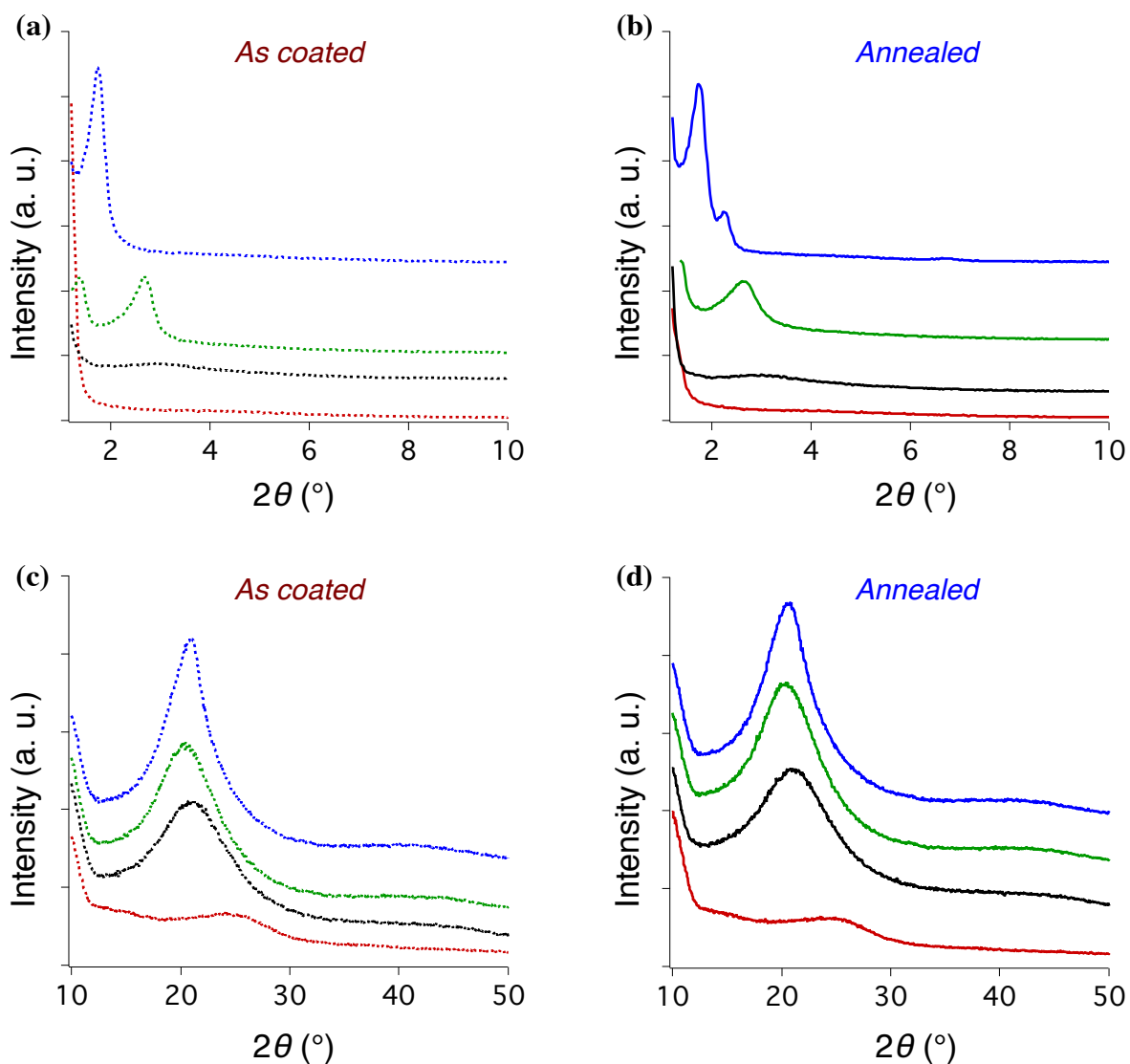


Figure S12: Thin-film XRD comparison of (a) as coated and (b) annealed film of PATA. Comparison of WAXD plots between (c) as coated and (d) annealed film of PATA. In both cases, there was no significant change in diffraction pattern indicating similar pattern of molecular stacking without/with thermal treatment.

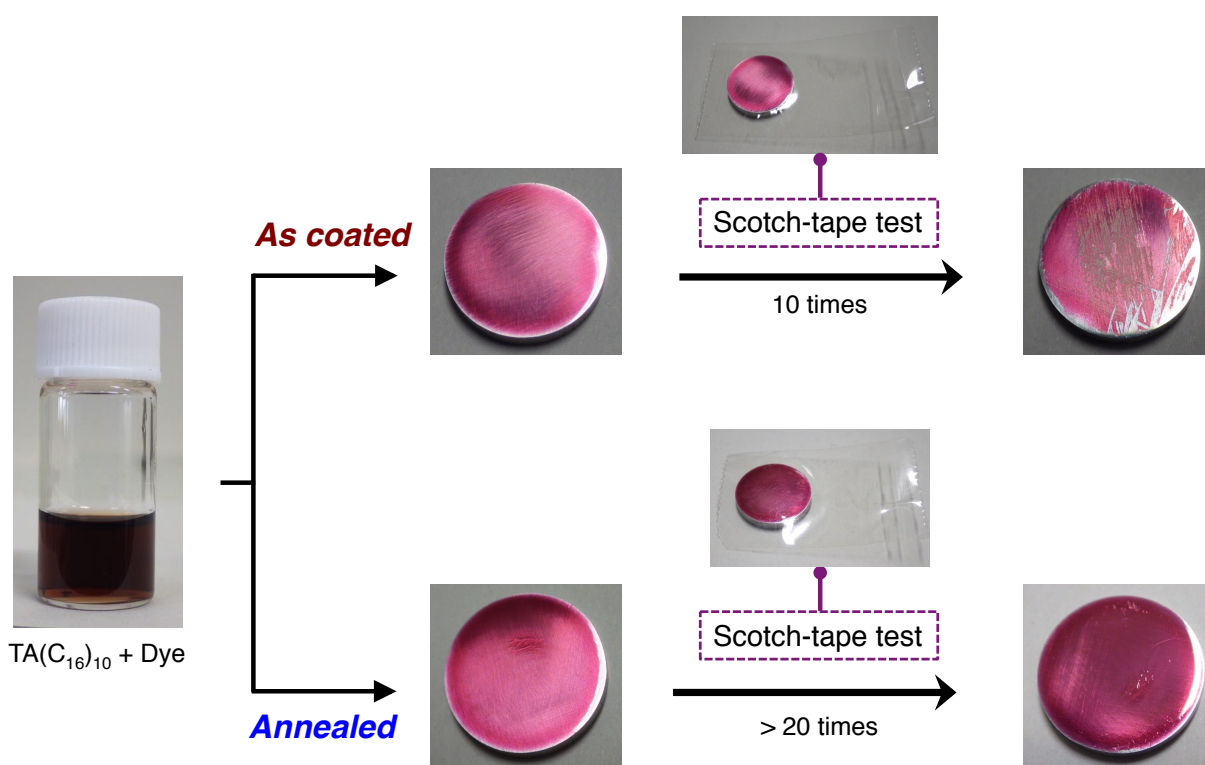


Figure S13: Although, AFM and SEM studies indicate good film-stability but we further verified mechanical stability of PATA coating by scotch-tape test and also effect of thermal treatment. Briefly to describe, few drops solution of TA(C₁₆)₁₀ was drop-casted on polished and well-cleaned magnesium alloy (AZ31) plate followed by drying under ambient condition or at 80 °C for 1 h. Small amount of Rhodamine B dye was added to visibly understand the difference. Afterthat, commercially available scotch-tape was repeatedly attached and peeled out using new one each time. We found major damage in the film without thermal treatment but annealed film was very stable upto many (>20) (de)attachment cycles. This result indicated thermal treatment enhances film stability and thus annealing was employed for all cases of anti-corrosion/bacterial study.

5. Anti-corrosion tests

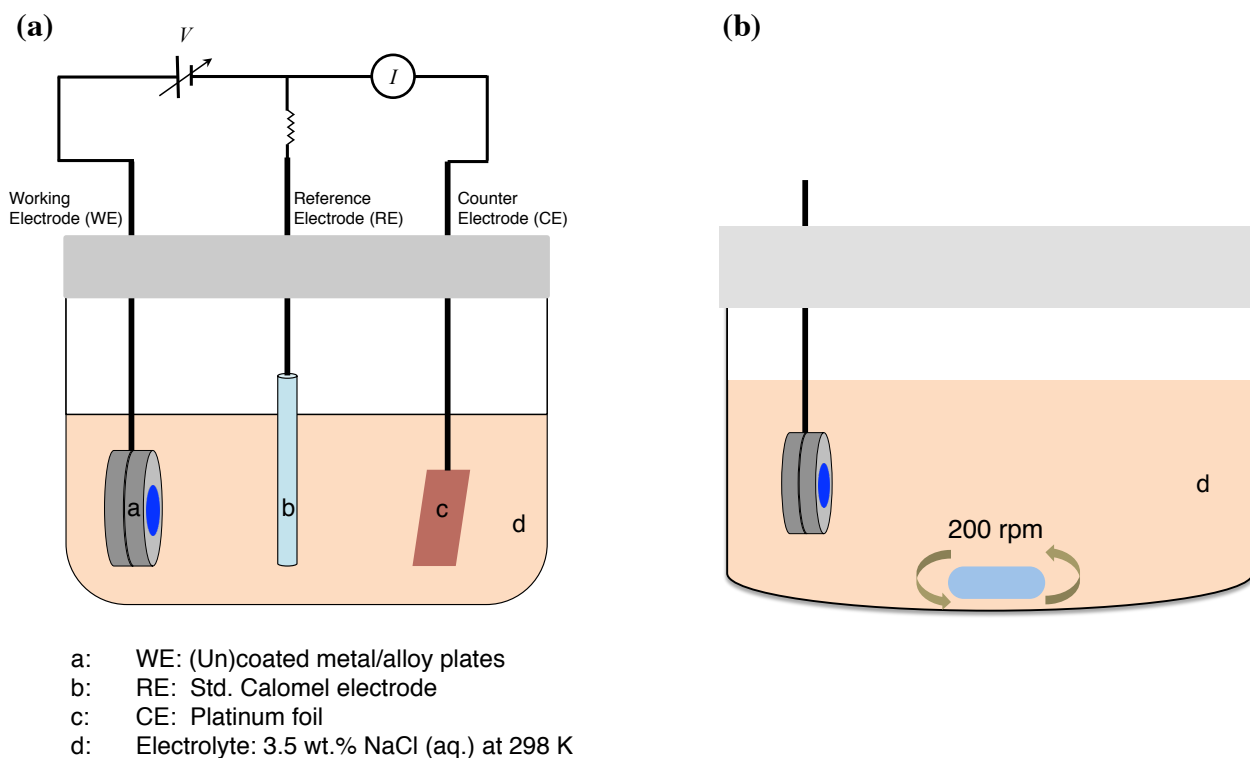


Figure S14: A simple schematic diagram of (a) electro-polarization test and (b) salt-water immersion test. All studies were performed at 298 K under air.

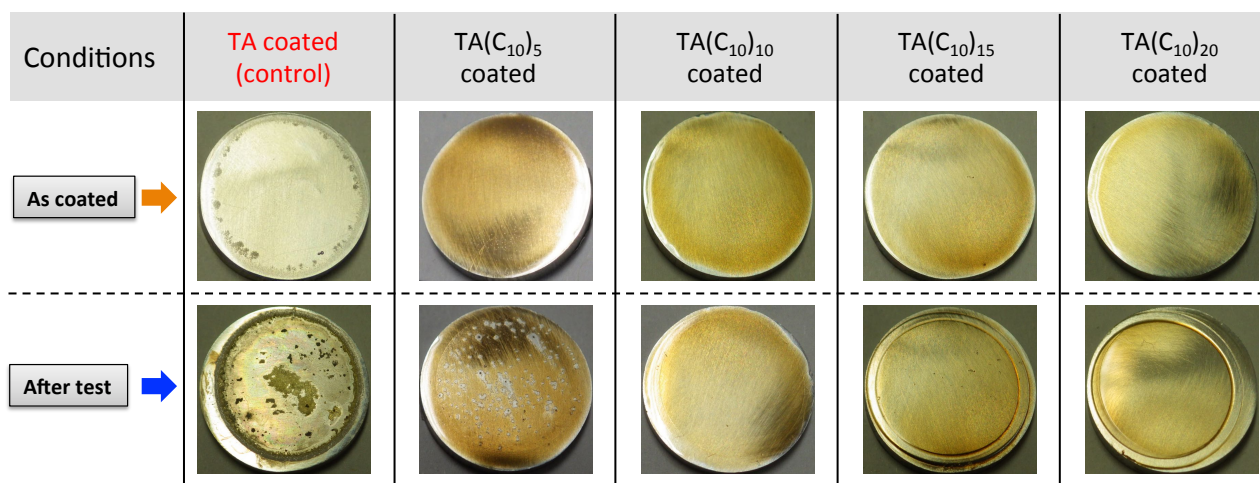


Figure S15: Photographs of different Mg alloy (AZ31) plates before and after electropolarization test. Plates were 15 mm in diameter. Obviously, TA coated (control) sample badly damaged after this test. Interestingly, there is a distinct variation among degree of substitution as revealed by this study. Penta-substitution, TA(C₁₀)₅ coated sample got severe damage (pinholes) during the test. Also, substitution more than ten (15, or 20) is not physically stable and become soft during the test. Therefore, the best choice of substitution was ten as TA(C₁₀)₁₀ coated sample was completely undamaged after the test. Considering, both electrochemical plots (Fig. 3) and visual inspections we conclude that deca-substitution gives perfect balance between anchoring aromatic hydroxyls and hydrophobic alkyl units to produce a well-adhered film and efficiently protect penetration of corrosive ions/ water molecules.

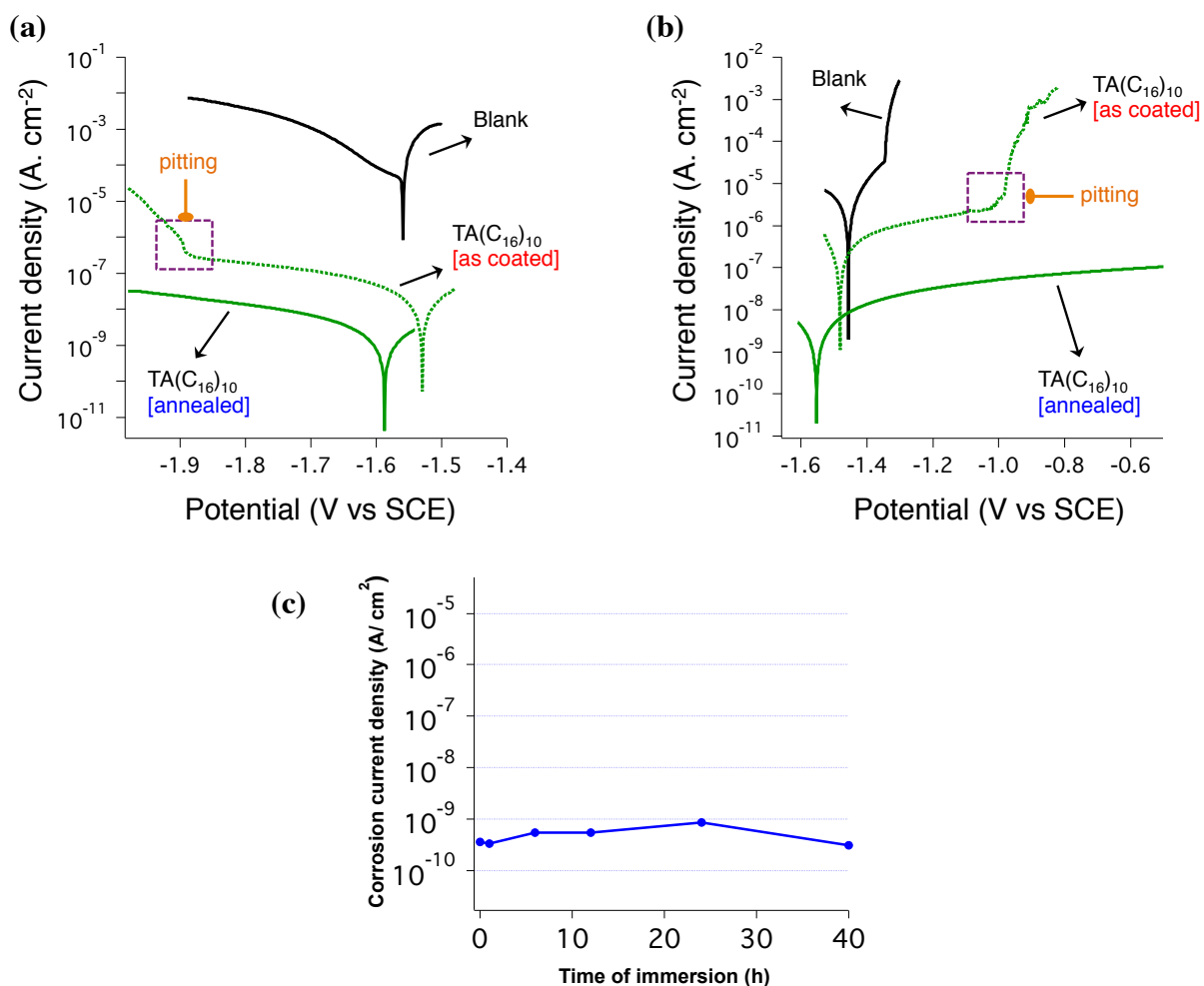


Figure S16: Effect of thermal treatment and time of immersion on electro-polarization test. (a) Cathodic, and (b) anodic current comparison among blank, as coated, and annealed samples. We discussed in earlier section that annealing has certain benefits to obtain a stable and firm film. However, to further demonstrate the relation between annealing and corrosion protection ability we compared corrosion current density (i_{corr}) between as coated and annealed film. Considering much less and smooth change of i_{corr} with potential sweep for annealed sample, it is obvious that thermal treatment has an important role for better corrosion protection. Fig. (c) demonstrates that long immersion time (upto 40 h) does not affect i_{corr} significantly, indicating long-lasting stability of our coating.

6. Anti-bacterial test:

As a test method, Japanese Industrial Standard (JIS Z 2801) was followed in this study.^b Three kinds of bacterial strains, [i] *Escherichia coli* (*E. coli*), [ii] *Staphylococcus aureus* (*S. aureus*), and (iii) *Methicillin-resistant S. aureus* (*MRSA*) were used in our study. Glass plate (5 x 5 cm²) was used as a substrate for coating. Minimum three tests were performed for each type of study.

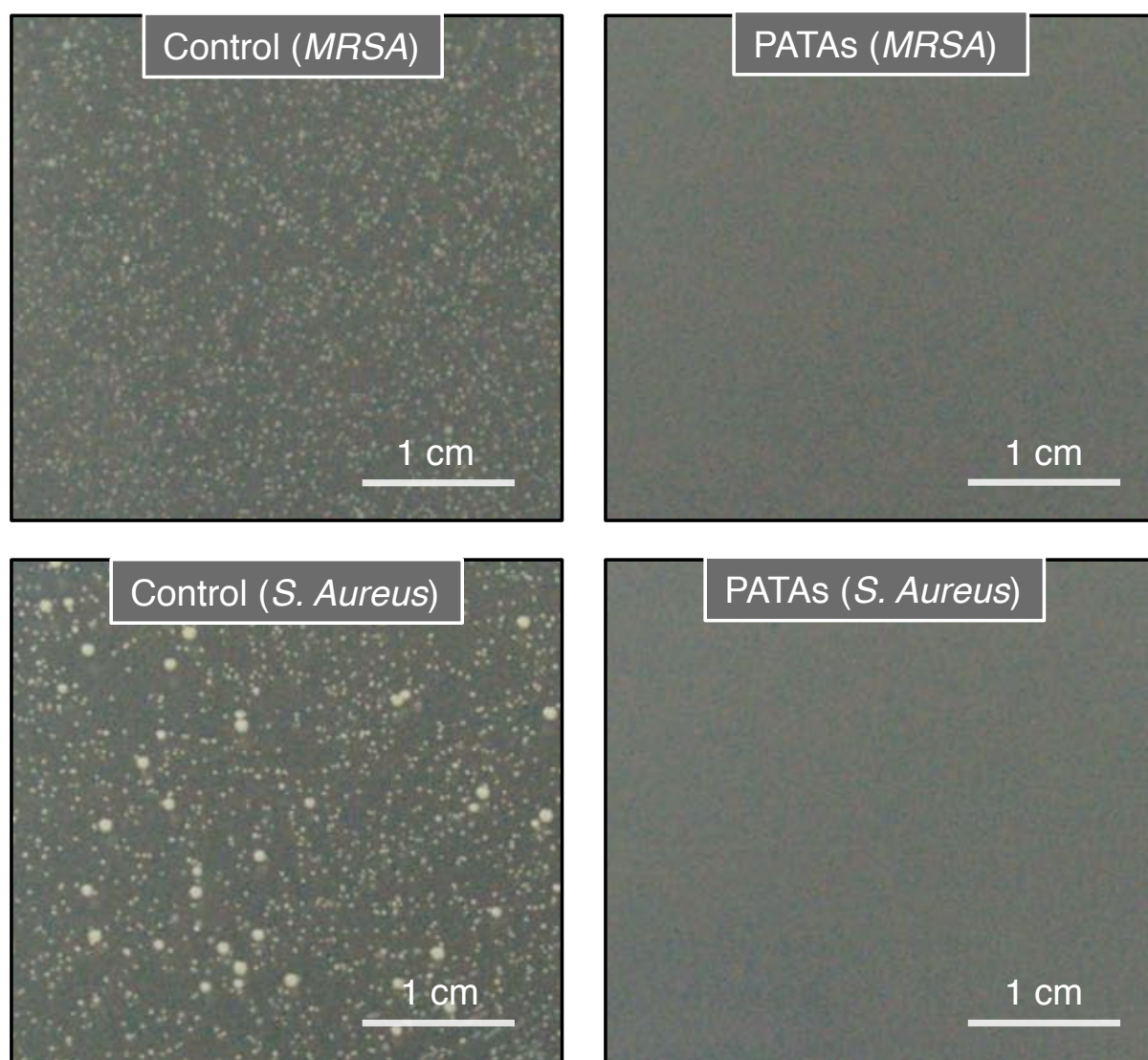


Figure S17: Photographs of different bacterial solutions after immersion of control (uncoated), and PATAs coated glass substrates. While bacterial colony remained unchanged or increased in control samples, PATAs samples completely killed the bacterial cells.

7. References

- a. Z. She, Q. Li, Z. Wang, L. Li, F. Chen and J. Zhou, *ACS Appl. Mater. Interfaces*, 2012, **4**, 4348.
- b. Japanese Industrial Standard/Antimicrobial products-Test for antimicrobial activity and efficacy JIS Z 2801:2010 (Japanese standard association 4-1-24, Akasaka, Minato-ku, Tokyo, 107-8440 Japan.)